Cogn Neurodyn (2009) 3:251–261
DOI 10.1007/s11571-009-9082-4

RESEARCH ARTICLE

On the synchrony of steady state visual evoked potentials and oscillatory burst events

Francois B. Vialatte · Justin Dauwels · Monique Maurice · Yoko Yamaguchi · Andrzej Cichocki

Received: 19 December 2008 / Revised: 9 March 2009 / Accepted: 9 March 2009 / Published online: 27 March 2009

Abstract In this paper, we investigate the large-scale synchrony of EEG oscillatory bursts, during stimulation by a flickering square of light. Whereas most studies focus on *averaged* raw EEG responses, this study considers oscillatory events within EEG of *single* trials, which leads to various new insights. We recorded EEG signals before, during and after stimulation by a flickering square of light in medium (16 Hz) and high frequency (32 Hz) ranges. Similar oscillatory bursts, to those observed in spontaneous EEG, can be found in single-trial synchrony of steady state visual evoked potentials (SSVEP). These bursts are extracted from the EEG of single trials using bump modeling. Stochastic event synchrony method is applied to those events, which quantifies synchronies of oscillatory bursts on a large-scale basis. Those oscillatory patterns have a significantly higher degree of co-occurrence during SSVEP, uncorrelated with ongoing signal synchrony. It means that EEG oscillatory patterns are presumably an outcome of brain activity, rather than a mere side effect of ongoing EEG. They undergo a consistent reorganization during visual stimulation, preferentially along the visual pathway, depending on magno or parvo stimulations. Flickering stimuli may induce some cognitive side-effects depending on the stimulation frequency.

Keywords SSVEP · Bump modeling · SES · Synchrony · Oscillations · Wavelet

F. B. Vialatte (✉) · M. Maurice · A. Cichocki
Lab. for Advanced Brain Signal Processing (L.ABSP),
RIKEN Brain Science Institute, 2-1 Hirosawa,
Wako-Shi, Saitama-Ken 351-0198, Japan
e-mail: fvialatte@brain.riken.jp

J. Dauwels
Laboratory for Information and Decision Systems,
MIT, Cambridge, MA, USA

M. Maurice · Y. Yamaguchi
Lab. for Dynamics of Emergent Intelligence (L.DEI),
RIKEN Brain Science Institute, Saitama, Japan

J. Dauwels
Laboratory for Mathematics in Imaging, Brigham & Women's Hospital, Department of Radiology, Harvard Medical School,
Boston, MA, USA

J. Dauwels
Amari Research Unit, RIKEN Brain Science Institute,
Saitama, Japan

Introduction

Oscillatory neuronal networks allow a unique interdisciplinary platform to study neurocognitive and dynamical phenomena (Rojas-Líbano and Kay 2008). EEG data, though of high relevance in cognitive research, poses a number of technical problems as it is very noisy and shows strong non-stationarities (Schinkel et al. 2007). Consequently, the structural organization and associated functional role of electroencephalographic (EEG) oscillations are still far from being completely understood. The complexity of EEG oscillations can be illustrated by the lack of consensus in EEG analysis methods (Kiebel et al. 2008). Brain oscillatory patterns have complex time, frequency and space structure. Synchrony among oscillating neural assemblies is a plausible candidate to mediate functional connectivity, and therefore to allow the formation of spatiotemporal representations (Le Van Quyen 2003; Cosmelli et al. 2007). Such neural structures can be considered as distributed local networks of neurons, transiently linked by reciprocal dynamic connections (Varela et al. 2001). Together, distant neural assemblies are involved in collective dynamics of

synchronous neuronal oscillations (Cosmelli et al. 2007), taking the shape of oscillatory patterns.

Cortical dynamics does not follow continuous patterns, but instead operates in steps, or frames (Freeman 2006): EEG is constituted of ongoing stationary oscillations, and non-stationary transient bursts. This bursts are local oscillatory events, present in single trials, and appearing as transient oscillatory synchronizations (TOS) or transient oscillatory desynchronizations (TOD). These synchronizations and desynchronizations correspond to the presence or absence of a coherent neural assembly, respectively (Başar et al. 1999). EEG activities are usually analyzed using either time or frequency representations of event related potentials (ERP), which can be interpreted as the reorganization of the spontaneous brain oscillations in response to the stimulus (Başar 1980; Başar et al. 1999). The origin of these ERP, obtained by signal averaging, is a matter of debate. Three main theories compete for the interpretation of what constitutes an ERP: additive effect of changes occurring in all trials, transient phase resetting of ongoing activity (Klimesch et al. 2007; Moratti et al. 2007), or baseline shift of ongoing activity (Nikulin et al. 2007). Nevertheless, ERP were observed in several studies to have visible outcomes even in single trials (Effern et al. 2000; Quiroga et al. 2001). In the present investigation, we are not interested in the averaged outcome of stimulations: the brain itself processes information at the single trial level (hence it processes TOS and TOD, not ERP).

In continuity with these theories, we would expect that organized oscillatory bursts (TOS and TOD) in EEG time–frequency activity (i.e., local synchronies) should play a specific functional role, distinct from the stationary ongoing EEG activity (activity not organized in bursts, representing 70–80% of the signal). Ongoing EEG was studied for years, and its high entropy suggests that it is likely to carry significant information. However, ongoing EEG and oscillatory burst were never compared on a large-scale basis (in distant electrodes). The first step to investigate this hypothesis is to demonstrate, using a well-know paradigm, that large-scale synchrony of ongoing EEG is consistently uncorrelated with large-scale synchrony of oscillatory bursts. This will be the purpose of our study: we investigate here the large scale dynamics of local synchrony patterns, during flickering light stimulation. During this stimulation, we will compare for each single trial these dynamics to those from ongoing activity. Our assumption is that these two activities will differ significantly.

Steady-state visual evoked potentials (SSVEP) is a well-known experimental paradigm in neuroscience. When averaged over many trials, SSVEP are characterized by constituent discrete frequency components remaining closely constant in amplitude and phase over a long stimulation time (Regan 1989). It is important to point out, however, that the discrete frequency component does not appear constant in *single* trials; it only appears so after *averaging* over a sufficient number of trials. In a single trial one observes bursts of oscillatory activities (cf. Fig. 2) during flickering light stimulation, similar to those that can be observed in spontaneous EEG.[1] In other sensory modalities, steady state potentials have also been documented: in the auditory system (Stapells et al. 1984); or similarly in the somatosensory system (Snyder 1992). Nevertheless, there is generally little known about the trial-by-trial detail of oscillatory patterns dynamics in SSVEP. Broadly speaking, investigations concerning the dynamics of SSVEP sources and topography are not sufficiently advanced (Nishifuji et al. 2006): studies in neuroscience use only classical signal processing methods to investigate the SSVEP responses—such as superposition, averaging, frequency analysis (narrow band Fourier power), or correlation analysis. Such methods are applied to the entire EEG signals. As both the ongoing EEG and oscillatory patterns are simultaneously analyzed, consequently the study of oscillatory patterns dynamics independently from ongoing EEG is not possible. Using recent modeling methods,[2] we will observe synchrony of single trials oscillatory bursts, uncorrelated with ongoing signal, in the SSVEP elicited by a flickering light stimulus. Our observations prove our assumption to be correct.

Methods

Whereas efficient tools for time–frequency analysis were used proficiently for implanted EEG (or ECoG, Chen et al. 2007), rest EEG (Vialatte et al. 2005; Chen et al. 2008), evoked potential or event-related responses investigation (Tallon-Baudry et al. 1996; Ohara et al. 2004; Vialatte et al. 2008c, 2009), time–frequency analysis of SSVEP were unfortunately seldom investigated (Cui and Wong 2006). Oscillatory patterns in the SSVEP elicited by a flickering light stimulus are extracted using a sparse "bump" model of the most prominent time–frequency oscillatory events (Vialatte et al. 2007, 2008a). Pairwise synchrony between all possible pairs of bump models is quantified with the method proposed in (Dauwels et al. 2007, 2009), referred to as stochastic event synchronization (SES). We then compare these results with a more general EEG synchrony measure using magnitude squared coherence (Kay 1998): coherence measures synchrony over the whole EEG signal, tacking into account both oscillatory bursts and ongoing EEG. All computations and statistical

[1] Spontaneous = in rest EEG (eyes opened or closed).

[2] This paper is the first report in journal, extending results that we previously presented in a conference (Vialatte et al. 2008b).

analysis were performed using MATLAB (The MathWorks, Inc.).

EEG recordings

The experiments were conducted in accordance with the Policies on the Use of Animals and Humans in Neuroscience Research, revised and approved by the Society for Neuroscience in January 1995, and in strict accordance with the Policy on Ethics approved by the Society for Neuroscience in November 1989, and amended in November 1993.

Human scalp EEG was recorded in a dark room, while the subject was exposed to flickering light. More precisely, the stimulus consisted of a single flashing white square of size 5 cm. The flickering frequency was constant (16 or 32 Hz) in order to produce a form of steady-state response of the human visual system (SSVEP). EEG data was recorded from 64 sites on the scalp, based on the extended 10–20 standard system. A Biosemi system with average reference was used. Sampling frequency was set to 2,048 Hz, with offline high pass filter with cut-off frequency 3 Hz, and low pass filter with cut-off frequency 45 Hz. Twelve second epochs were recorded with a 64 channel montage. A single trial had the following structure: before stimulation (3 s, labeled thereafter "Before" period), during stimulation (5 s, labeled thereafter "During" period) and a post-stimulation period (4 s labeled thereafter "After" period), during which EEG resumed to the baseline activity. A total of 102 records, 51 with 16 Hz stimulation and 51 with 32 Hz stimulation, were recorded. Data were obtained from a single subject.

Time–frequency sparsification

The purpose of this step is to extract local synchrony patterns. These patterns are to be found in the time–frequency structure of EEG dynamics oscillations—time–frequency analysis is especially suitable for this task (Le Van Quyen and Bragin 2007). After time–frequency analysis, oscillatory bursts are extracted using bump modeling, which extracts only the most prominent and organized time–frequency patterns (Vialatte et al. 2007; Dauwels et al. 2008). Bumps were extracted using the ButIf toolbox (Vialatte et al. 2008a).

As a first step, wavelet time–frequency maps are computed using complex Morlet wavelets. The (continuous) wavelet transform $\mathbf{W}$ of a time series $\mathbf{x}$ is obtained as:

$$\mathbf{W}(k,s) \stackrel{\Delta}{=} \sum_{l} \mathbf{x}(l)\psi^{*}\left(\frac{l-k}{s}\right),$$

where $\psi(k)$ is the (complex) "mother" wavelet, s is a scaling factor, and * stands for complex conjugate. In this paper, we used the complex Morlet wavelet:

$$\psi(k) = A \cdot \exp\left(\frac{-k^2}{2\sigma_t^2}\right) \cdot \exp(2i\pi f_0 k),$$

where σ_t^2 and f_0 jointly determine the number of oscillations in the wavelet. The complex Morlet wavelet results in the optimal resolution in time and frequency; it has also proven to be well-suited for EEG signals (Tallon-Baudry et al. 1996; Ohara et al. 2004; Herrmann et al. 2005; see also Le Van Quyen and Bragin 2007 for review). Here, time–frequency representations were restricted to the frequency ranges of SSVEP, i.e., 15–17 Hz (for 16 Hz stimulation) or 31–33 Hz (for 32 Hz stimulation), with adequate time and frequency borders for bump modeling (Vialatte et al. 2007; Dauwels et al. 2008). Epochs were analyzed before, during and after stimulation. Frequency dependent z-score normalization (Browne and Cutmore 2004; Vialatte et al. 2009) was applied comparatively to the pre-stimulus period of each trial:

$$\mathbf{z}(f,t) = \frac{\mathbf{W}(f,t) - \mu_f}{\sigma_f}$$

where μ_f and σ_f are the mean and standard deviation, respectively, of the wavelet map $\mathbf{W}$, computed over the pre-stimulus period at frequency f. The resulting z-score maps $\mathbf{z}(f, t)$ are approximated as a sum $\mathbf{z}_{\text{bump}}$ of basis functions b ("bumps") with parameters θ_k (for more details about bump modeling, see Vialatte et al. 2007):

$$\mathbf{z}(f,t) = \mathbf{z}_{\text{bump}}(\theta) = \sum_{k=1}^{N_b} b(\theta_k),$$

where $\theta = (\theta_1, \theta_2, \ldots, \theta_{N_b})$. This decomposition represents the most salient events in the z-scored map $\mathbf{z}(f, t)$; these can most probably be attributed to the local organization of brain activity (local synchrony). We used half ellipsoid basis functions b, the parameters θ_k are vectors of five parameters: position in time and frequency, width in time and frequency, and amplitude. After bump modeling, the 64 electrodes were clustered into a set $\mathbf{A}$ of nine areas (occipital, parietal left and right, temporal left and right, central, frontal left and right, and prefrontal electrodes) by means of the aggregation algorithm described in (Vialatte et al. 2007). This reduces the complexity of data analysis and increases the robustness of our results against statistical fluctuations, since we consider fairly large brain regions. Moreover, this strategy reduces considerably the risk of measuring volume conduction effect instead of synchrony.

Stochastic event synchrony

Next we need to evaluate in each single trial the large-scale synchrony of the oscillatory patterns extracted. We determine the similarity of all pairs ($\mathbf{A_i}$, $\mathbf{A_j}$) of aggregated bump

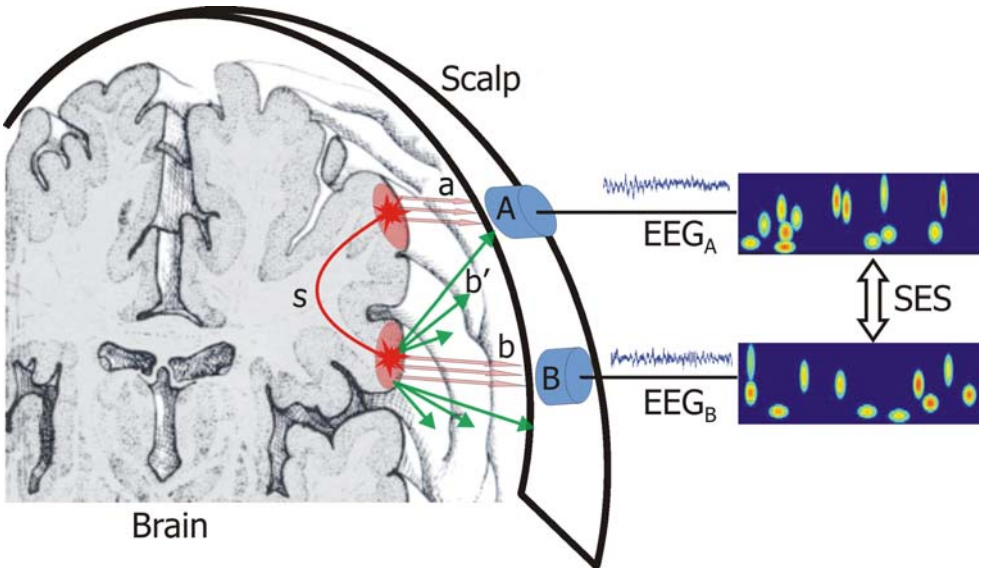

Fig. 1 Stochastic event synchrony (*SES*). Two EEG electrodes (**A**, and **B**) record brain activity (EEG_A and EEG_B) in their vicinity (a and b) together with activity from distant electrodes (b'). Locally synchronous bursts of oscillatory activity appear as bumps in the time–frequency domain. We are interested in the synchrony (s) between those events; we quantify this synchrony by means of SES

models (Fig. 1). To this end, we apply the stochastic event synchrony method (SES; Dauwels et al. 2007), which quantifies to which extent two bump models $\mathbf{z_A}$ and $\mathbf{z_B}$ can be aligned. SES consists of the triple (ρ, δ, σ); these three numbers jointly describe the similarity of two bump models:

- a fraction ρ of bumps appear in one bump model but not in the other ("spurious" bumps).
- Other bumps are present in both models at slightly different positions on the time–frequency map ("non-spurious bumps").
- We denote by δ and σ the average delay between pairs of non-spurious bumps (global jitter) and the standard deviation of this offset (local jitter), respectively.

The solution is determined by maximum a posteriori estimation.

In our previous investigation (Vialatte et al. 2008b), we used the actual number of bumps modeled before and during stimulation, and obtained similar results. The observed effect could, however, be due to the increase of the number of bumps, biasing the SES computation. In order to avoid such bias, in the present study, SES was applied with a constant number of bumps for all conditions (the seven-first bumps per period). The observed results are robust to parameter changes.[3]

Statistical analysis

All statistics were corrected using a Bonferroni correction for tests (see e.g., Vialatte and Cichocki 2008). We computed the general average of all pairwise synchrony measures (SES measures and coherence measures), for each experimental conditions (before, during, after, for 16 or 32 Hz stimuli). This provided information of the general synchrony depending on the experimental context—answering the question: "is there synchrony during SSVEP?" We used this measure in order to compare synchronization effects between experimental conditions (Before vs. During, Before vs. After, During vs. After) using a Wilcoxon test. A similar approach was used with ongoing synchrony (coherence measures).

Afterwards, we analyzed the synchrony for the nine brain areas **A** (aggregation of the bump algorithm), using a Wilcoxon test to compare all pairwise SES synchrony measures ($\mathbf{A_i}$, $\mathbf{A_j}$) between all the areas. This provided information about the brain topography of the synchronization effect, for SSVEP experimental conditions (Before vs. During, During vs. After)—answering the question: "which brain areas are synchronized during SSVEP stimulation?" This result was afterwards compared with the topography of ongoing synchrony (coherence measure—the algorithm used to regroup the coherence measure in nine brain areas **B** can be found in annex). This strategy if used to compare the topography of the effect.

A comparison with surrogate data was necessary in order to control if the observed effect is an artifact of the method. We generated 1,000 surrogate data sets by the following two-step procedure: first a trial is selected randomly, next the nine aggregated bump models of that trial are shuffled, more precisely, the timing of the bumps in those models is chosen randomly, uniformly within the support of those models, the four other bump parameters are left unchanged. We applied SES to each of those 1,000 surrogate data sets resulting each time in parameters ρ, δ, and σ. We then compared the SES parameters obtained from the real data to the parameters of the 1,000 surrogate

[3] Using less optimized parameters, we could observe lower P values—they still remained highly significant ($P < 0.01$).

data sets (using general averages of the pairwise synchrony measures).

Ongoing synchrony

We intend to measure how the ongoing EEG (the part of signal rejected during bump modeling) is synchronized. Because we extract the most prominent activities of EEG signals during bump modeling, the best comparative synchrony measure is magnitude squared coherence (Kay 1998), a measure large-scale synchrony when applied to scalp EEG (see e.g., Duckrow and Zaveri 2005). The magnitude squared coherence $\mathbf{C_{xy}}$ estimate is a function of frequency with values between 0 and 1 that indicates how well two time series x and y corresponds one to another at each frequency f. The coherence is a function of the power spectral density ($\mathbf{P_{xx}}$ and $\mathbf{P_{yy}}$) of x and y and the cross power spectral density ($\mathbf{P_{xy}}$) of x and y:

$$\mathbf{C_{xy}}(f) = \frac{\left|\mathbf{P_{xy}}(\mathrm{f})\right|^2}{\mathbf{P_{xx}}(f)\mathbf{P_{yy}}(f)}$$

Results

We observed that the z-score maps $\mathbf{z}(f, t)$ contain oscillatory bursts before, during, and after flickering stimulation (Fig. 2). In other words, spontaneous EEG as well as SSVEP both contain non continuous oscillatory events. In SSVEP (during stimulation) there tend to be more of these events than in spontaneous EEG. In the transient regime after stimulation, the number of events gradually decreases.

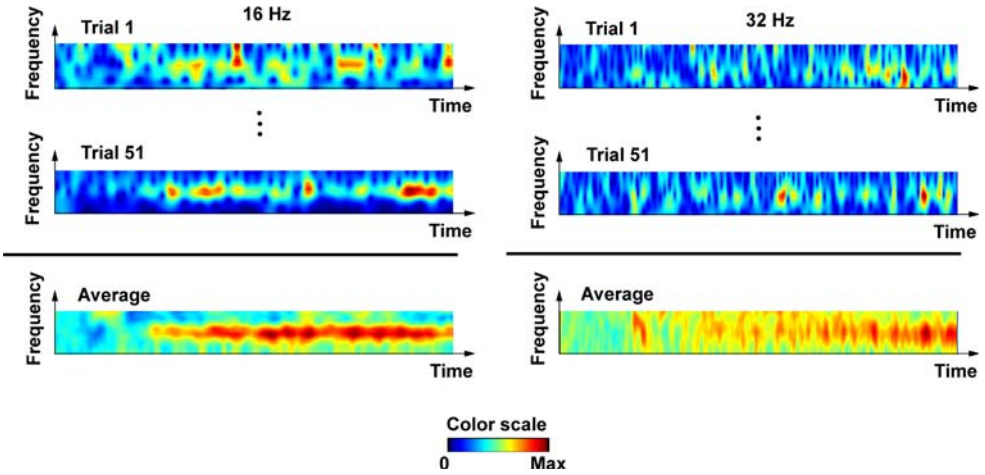

Fig. 2 Example of wavelet time–frequency representation of SSVEP in occipital area (channel O_2). The difference between single trials (with oscillatory patterns) and average of 51 trials (with almost continuous activity) is obvious in both 16 Hz (*left*) and 32 Hz (*right*) SSVEP

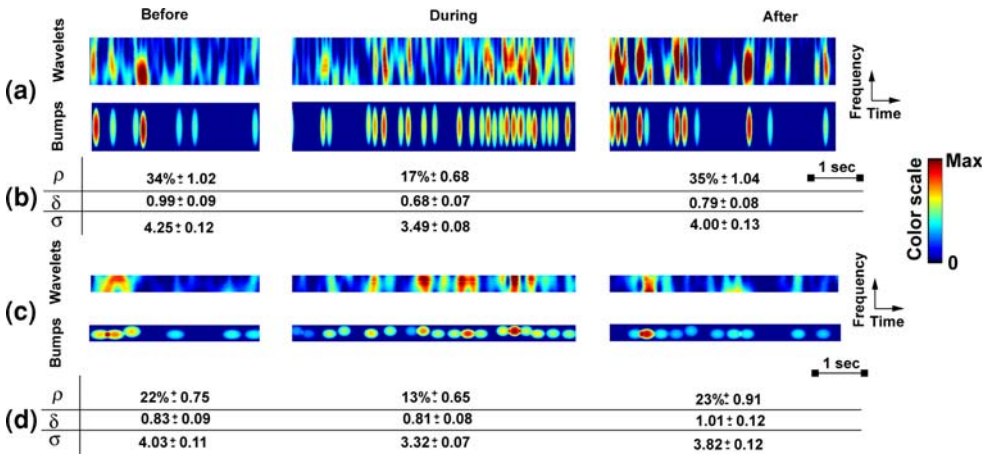

Fig. 3 Application of bump modeling and SES to SSVEP signals, compared with magnitude squared coherence. Bumps are modeled with central frequencies within 1 Hz of the stimulation frequency. **a** z-scored wavelet transform $\mathbf{z}(f, t)$ (26–38 Hz) with reference in the "Before" period (*top*) and bump modeling (*bottom*) of a typical signal with SSVEP at 32 Hz (single trial). **b** SES parameters computed trial-by-trial for all signals at 32 Hz. **c** z-scored wavelet transform (13–19 Hz) with reference in the "Before" period (*top*) and bump modeling (*bottom*) of a typical signal with SSVEP at 16 Hz. **d** SES parameters computed trial-by-trial for all signals at 16 Hz (single trial)

We determined EEG synchrony for each of the three conditions (before, during, and after stimulation) by means of magnitude square coherence and SES (Fig. 3). The condition pairs "Before vs. During" and "During vs. After" yield significant P values ($P < 0.01$, Wilcoxon test) for magnitude squared coherence, ρ and σ. Those three measures indicate that the synchrony is larger *during* stimulation than before or after, more precisely, during stimulation the magnitude squared coherence significantly increases; on the other hand, ρ and σ decrease significantly (Fig. 4). The parameter δ also decreases during the flickering stimulation, but not significantly ($P = 0.08$). Note that σ captures fluctuations "within" a trial, whereas the distribution of δ reveals fluctuations "from trial to trial".

The parameter ρ measures synchrony in a similar way as magnitude squared coherence—we could expect these two measures to report correlated results if oscillatory bursts and background EEG shared the same functional role. We compared ρ values with magnitude squared coherence, no correlation was found in any condition (Table 1). This is illustrated by the scatter plots of the co-occurrence parameter against magnitude squared coherence during stimulation period (Fig. 5).

We computed the SES parameters for the surrogate data sets. The parameter δ has about the same values for the real and surrogate data; in other words, this parameter turns out to be of little relevance for this study. The parameters σ and ρ have clearly larger values for the surrogate data ($P \ll 0.01$ with Mann–Whitney test) in each of the three conditions (Before, During and After). This shows that the organization of EEG oscillatory events is non-trivial and interesting. Moreover, also for the surrogate data sets, the parameters ρ and σ decrease significantly during stimulation, but the difference is less strong than in the real data. Therefore, the reduction in ρ and σ cannot only be explained by the larger number of oscillatory events during stimulation, it is due to an increase in synchrony of the events (this effect cannot be explained by changes in oscillatory power).

We studied the spatial organization of SES co-occurrences in the nine areas, showing the most significant changes in the ρ parameter: we compared the pairwise synchrony ($\mathbf{A_i}$, $\mathbf{A_j}$) between each of the set of nine brain areas $\mathbf{A}$ of bump aggregation (Fig. 6). The propagation of oscillatory burst co-occurrence during flickering stimulation depends on the stimulation frequency (16 or 32 Hz). After stimulation, the EEG oscillatory activity resumed progressively its normal pace, but with a preference towards trans-hemispheric (hemisphere to hemisphere) reduction of co-occurrence.

This spatial organization was then compared with the pairwise magnitude squared coherence ($\mathbf{B_i}$, $\mathbf{B_j}$) between all brain areas of the set $\mathbf{B} \sim \mathbf{A}$. A distinct distribution is shown by magnitude squared coherence (Fig. 7). The propagation of oscillatory burst co-occurrence during flickering stimulation depends on the stimulation frequency (16 or 32 Hz), but in very similar locations. After stimulation, the EEG oscillatory activity resumed progressively its normal pace, but with a preference towards trans-hemispheric (hemisphere to hemisphere) reduction of synchrony, similar to what was observed with SES. This means that after SSVEP, oscillatory activity remains coordinated after the stimulation ends for a few seconds, but with two distinct dynamics in both hemispheres.

Fig. 4 Boxplots of the three SES parameters. "*" Represents ▶ significant ($P < 0.01$) differences using Wilcoxon test with Bonferroni correction. "+" represent outliers

Discussion

During a flickering light stimulation, we compared, for each single trial, organized dynamics against those from background (disorganized) activity. Our assumption was that these two activities will differ significantly. We have shown using SES that local oscillatory bursts display significant patterns of large scale synchrony during flickering light stimulation. We measured the background EEG synchrony using a well-known measure, magnitude square coherence.[4] This synchrony significantly differs from background activity as shown by their absence of correlation (Table 1; Fig. 5); or by their differing spatial distributions (Fig. 7 compared to Fig. 6). This proves our primary assumption to be right.

We also showed that single trials of SSVEP are composed by successions of rhythmic patterns. Earlier investigations (Cui and Wong 2006) also revealed such patterns in the time–frequency maps of single-trial EEG during stimulation with flickering light. In contrast, if one averages the EEG over a sufficient number of trials, one can observe more constant and stable activity on the time–frequency map, especially around the stimulation frequency. While the overall oscillatory organization of EEG remains normal during stimulation, a larger number of oscillatory events is observed. In other words, we can still observe segregated bursts of activity, but these oscillatory bursts occur more frequently than in spontaneous EEG. Furthermore, the synchrony of the oscillatory events

[4] Comparisons of magnitude square coherence between rest and stimulus conditions might be inaccurate if the signal to noise ratio (SNR) is different in both conditions (Nunez and Srinivasan 2006). In our case, however, we are not interested in proving the presence of synchrony ("if" question) but in its location ("how" question). We know that SSVEP propagates; we consequently assume that background synchrony is indeed present.

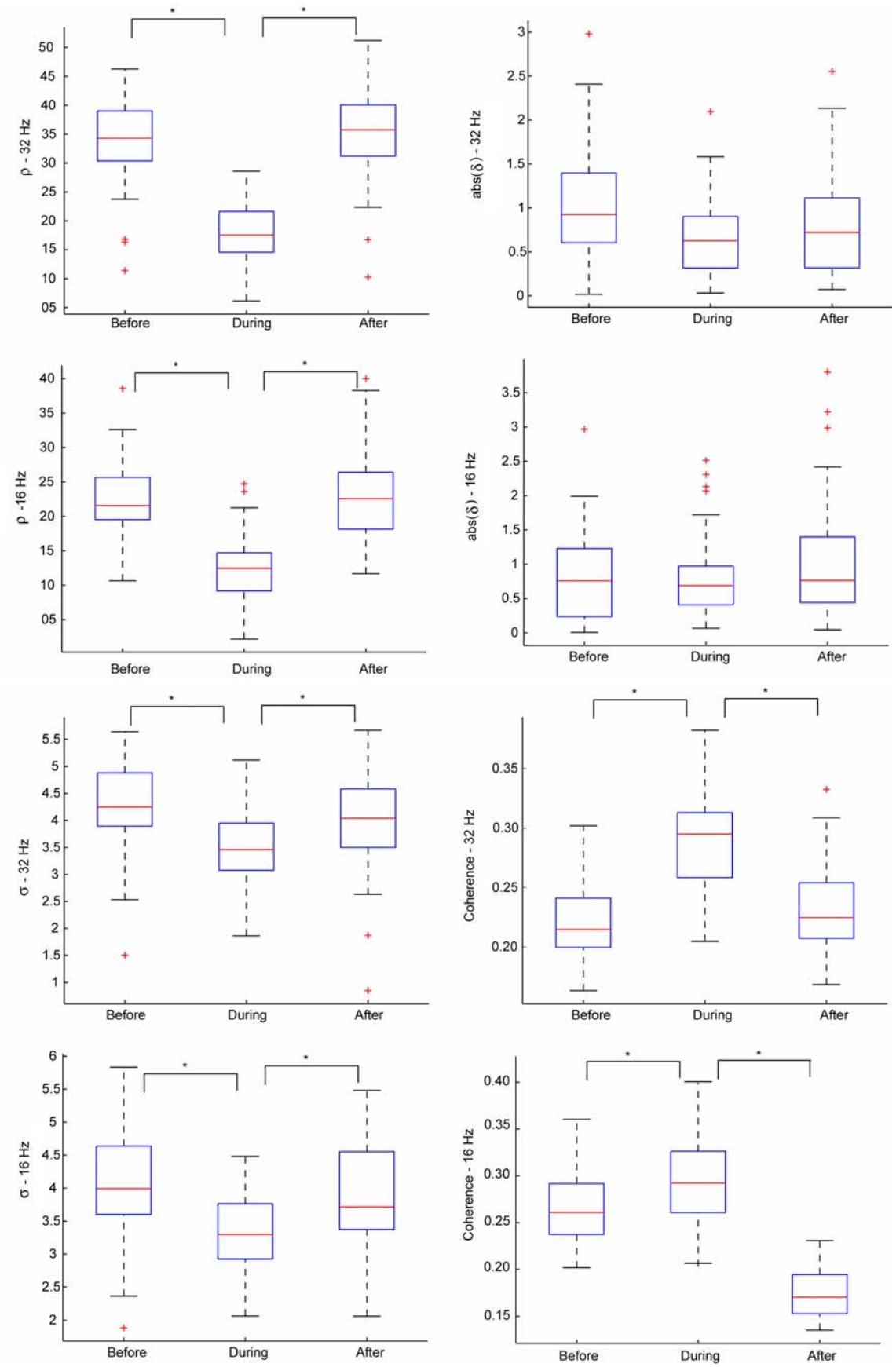
ρ - 32 Hz
abs(δ) - 32 Hz
ρ -16 Hz
abs(δ) - 16 Hz
σ - 32 Hz
Coherence - 32 Hz
σ - 16 Hz
Coherence - 16 Hz
Before
During
After
*

Table 1 Correlation test between ρ and coherence

Condition	Pearson R	P values ($df = 49$)
16 Hz, before	0.07	>0.10
16 Hz, during	0.21	>0.10
16 Hz, after	0.09	>0.10
32 Hz, before	0.16	>0.10
32 Hz, during	0.14	>0.10
32 Hz, after	0.06	>0.10

No significant effect is observed (P values always >0.10, even without Bonferroni correction)

With $df = 49$, R should be above 0.279 to observe a significant effect (if using Bonferroni correction, $R > 0.361$ at least)

increases during stimulation. These observations can be interpreted as:

- a reorganization of the oscillatory patterns in the visual system by the flickering stimulation, which propagates from the visual areas to the whole brain.
- Or a quantitative increase of the brain activity at the SSVEP frequency, coupled with (and modulated by) other independent sequences of ongoing brain activity, engendering an apparent synchrony of oscillatory patterns.

The former is more likely to be true, as modulation by different brain sources would most likely change somehow the dynamics, which we did not observe. The interpretation of reorganization is also consistent with the generally observed effect of phase resetting associated with visual evoked potentials (Ding et al. 2006). If we make the common assumption that oscillations and long distance synchrony both play key roles for cognition (Varela et al. 2001; Cosmelli et al. 2007), we can conjecture from these results that SSVEP stimuli might induce cognitive side-effects, depending on their frequency. For instance, subjects often complain that SSVEP stimuli are disturbing, and sometimes fall asleep during recording sessions—could these effects be attributed to the perturbation of brain large-scale synchrony?

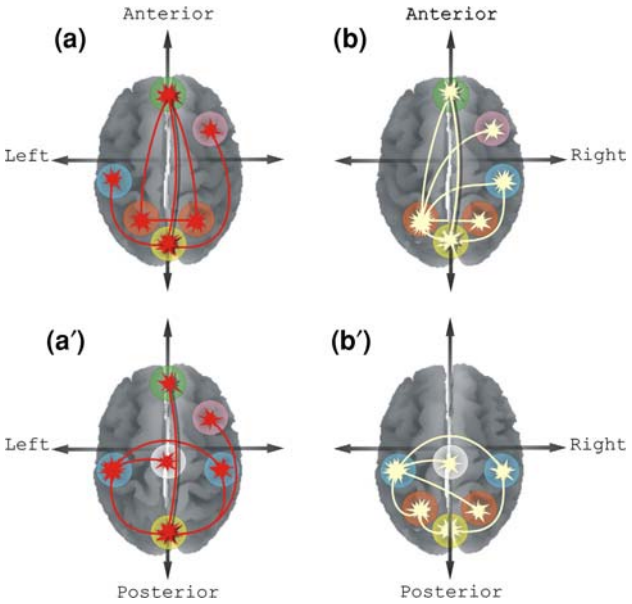

Fig. 6 Preferential pathway of oscillatory burst co-occurrences. We can observe the difference between recording periods: *before* versus *during* stimulation at 32 Hz (*a*) and 16 Hz (*a*′) and *during* versus *after* stimulation at 32 Hz (*b*) and at 16 Hz (*b*′). *On the left, lines* represent an increase in synchrony between the oscillatory events during stimulation compared to the baseline EEG. *On the right, lines* represent a decrease in oscillatory event synchrony in the period after stimulation. For both frequencies under consideration, stimulation induces a significant increase in event synchrony (*a*, *a*′) between the occipital areas (*lowermost zone*) on the one hand and the frontal (*top-right zone*) and orbitofrontal areas (*uppermost zone*) on the other hand. The details of this path depend on the frequency: for SSVEP at 32 Hz, the privileged path goes through parietal areas (*bottom-left and bottom-right zones*) whereas for SSVEP at 16 Hz it goes through temporal areas (*leftmost and rightmost zones*). After stimulation (*b*, *b*′), the extinction of the activity follows preferentially a trans-hemispheric decrease

The reorganization of oscillatory events propagates preferentially through the visual pathway (Fig. 8); the 32 Hz stimulation activates preferentially the magnocellular pathway, while the 16 Hz stimulation activates preferentially the parvocellular pathway. This is consistent with what we expected, as high frequency flickering stimuli

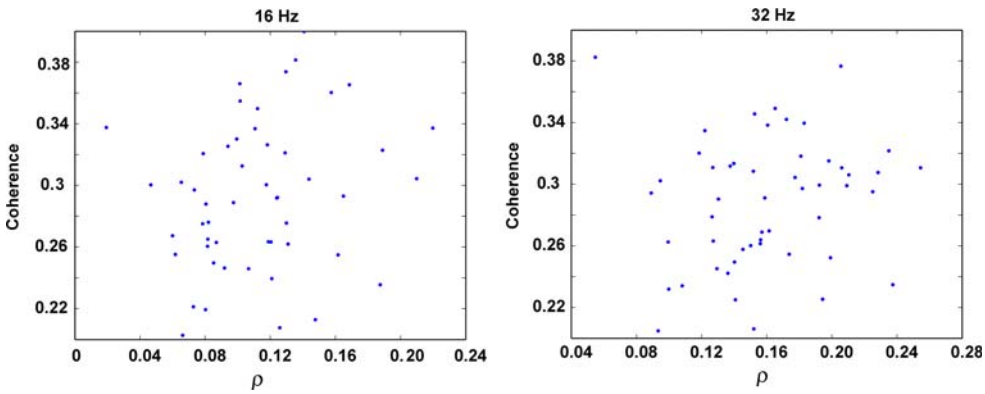

Fig. 5 Scatterplot of SES co-occurrence measure against magnitude squared coherence during flickering light stimulation. There are obviously no correlation between these measures

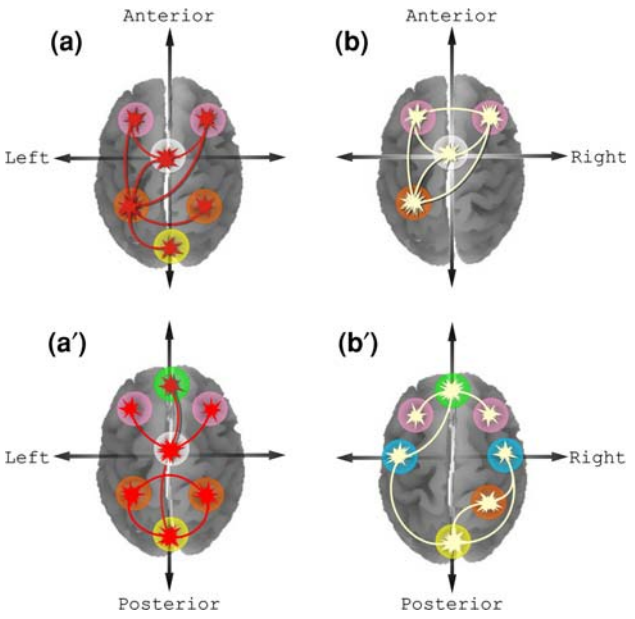

Fig. 7 Preferential pathway of EEG background synchrony (using coherence measures). We can observe the difference between recording periods: *before* versus *during* stimulation at 32 Hz (*a*) and 16 Hz (*a*′) and *during* versus *after* stimulation at 32 Hz (*b*) and at 16 Hz (*b*′). *On the left, lines* represent an increase in synchrony between the oscillatory events during stimulation compared to the baseline EEG. *On the right, lines* represent a decrease in oscillatory event synchrony in the period after stimulation. For both frequencies under consideration, stimulation induces a significant increase in coherence (*a*, *a*′), very similar in location for both conditions (*a* vs. *a*′). After stimulation (*b*, *b*′), the extinction of the activity follows preferentially a trans-hemispheric decrease

tend to elicit responses biased towards the magnocellular pathway (see e.g., Kim et al. 2007). However, this does not match well with the classical picture about the propagation of SSVEP in the brain. The complex spatial distributions of SSVEP observed in brain imaging were until now attributed to standing and traveling waves (Burkitt et al. 2000) or by sequences of source activation (e.g., Di Russo et al. 2007); it is noteworthy that these two classical theories do not necessarily exclude each other, they are rather complementary (Thorpe et al. 2007). The theory of source sequences explains the complex patterns by alternative activations in different brain areas; on the other hand, the theory of traveling and standing waves theory explains the complex patterns by the complex superposition of electrical waves. Our results suggest a third complementary theory. Contrary to usual studies, we investigate the dynamics of oscillatory bursts in the EEG and neglect the background EEG. We can assume that oscillatory bursts in EEG arise from brain mechanisms organized in frames (Freeman 2004), which are characterized by non-stationary state transitions. As we have shown, background EEG did not follow a consistent reorganization following the visual pathway (Fig. 7 compared to Fig. 6). We would therefore expect either:

– Weakly significant and trial-dependent effects of bump co-occurrence between different brain areas *if* we assume that oscillatory peak patterns are a side-effect of the background activity.

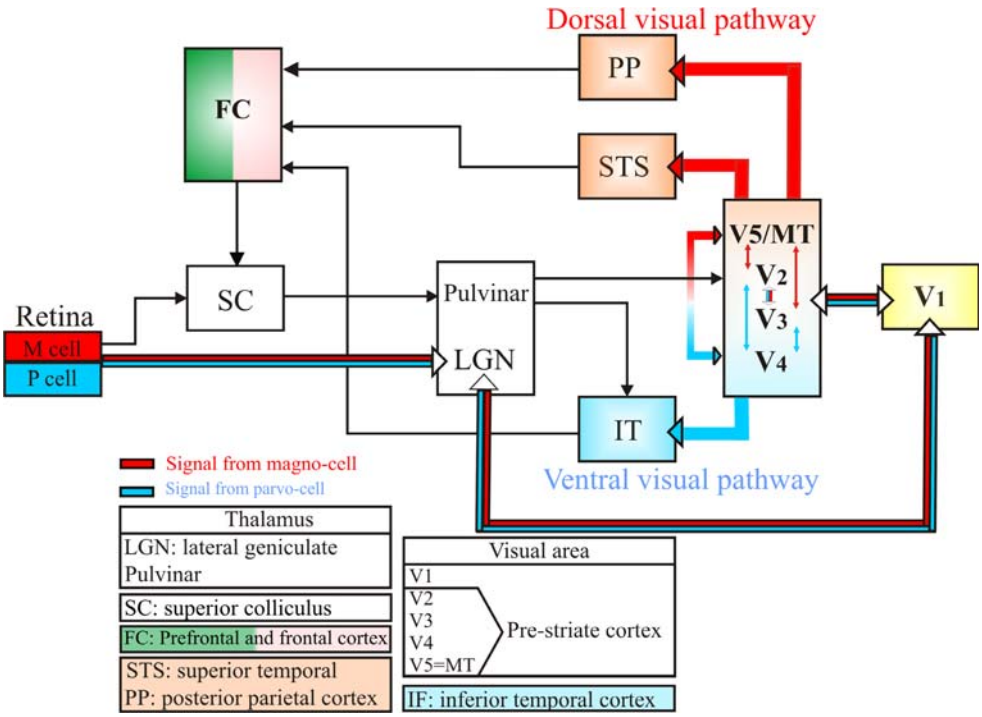

Fig. 8 Simplified illustration of the visual parvocellular and magnocellular pathways. Magnocellular pathway follows a dorsal propagation, whereas parvocellular pathway follows a ventral propagation. The *regions* approximately correspond to those of Figs. 6 and 7

– A consistent reproducible flow *if* we assume that oscillatory peaks and background activity are only weakly coupled

Our observations seem to support the second hypothesis; we observed a consistent reorganization of the EEG oscillatory events along specific visual pathways. This hypothesis does not contradict classical theories. Indeed, we wish to point out that bump modeling removes most of the EEG background signal. Sequences of source activations and/or traveling and standing waves may occur in the background activity. On the other hand, oscillatory events are to some extent decoupled from the background activity and are preferentially reorganized along the visual pathway.

As a final remark, the reader should bear in mind that the above effects were reported using one subject. Because we checked using surrogate data that our results are not spurious, and because we constrained the number of bump as compared to what we reported in (Vialatte et al. 2008b), this is a sufficient (as we investigate here a typical, and not a quantitative aspect of EEG, see e.g., Friston et al. 1999) proof that EEG oscillatory bursts and EEG background[5] activity are functionally discorrelated. On the contrary, the reported effect of visual pathway propagation could vary depending on subjects. Furthermore, the propagation effect is observed only at the scalp level, because bump modeling does not allow yet the possibility to compute more reliable source reconstructions. This final point has to be understood as explanatory (it shows that our results are biologically plausible) and illustrative: this effect has to be confirmed with more subjects, and more technical investigations, which will be the object of our future reports.

Acknowledgments The authors express their thanks to Pr. Remi Gervais and Pr. Gerard Dreyfus for their contribution in the early developments of bump modeling. They are grateful to participants the RIKEN Symposium "Brain Activity and Information Integration" (September 2007, RIKEN, Saitama, Japan), and the NIPS Workshop "Large-Scale Brain Dynamics" (December 2007, Whistler, Canada) for numerous inspiring questions and comments about bump modeling and SES. Justin Dauwels is in part supported by the Henri–Benedictus Fellowship from the King Baudouin foundation and a fellowship from the Belgian American Educational Foundation (BAEF). Dr. T. M. Rutkowski recorded SSVEP data and helped for preliminary investigations. Monique Maurice is supported by the JSPS fellowship P-08811.

Appendix

We regrouped all pairwise coherence measures $\mathbf{C_{xy}}$ between all electrodes x and y, into nine pre-defined set $\mathbf{B}$ of brain areas ($\mathbf{B_1}$ = occipital, $\mathbf{B_2}$ = frontal left, $\mathbf{B_3}$ = frontal right, $\mathbf{B_4}$ = temporal left, $\mathbf{B_5}$ = central, $\mathbf{B_6}$ = temporal right, $\mathbf{B_7}$ = parietal left, $\mathbf{B_8}$ = parietal right, $\mathbf{B_9}$ = occipital) corresponding to the nine zones used for bump modeling aggregation. Each $\mathbf{B_i}$ encompasses a set of N_i electrodes; the same electrodes that were used for bump modeling aggregation (In other words, $\mathbf{B_i} \sim \mathbf{A_i}$). For each pair of brain areas ($\mathbf{B_i}$, $\mathbf{B_j}$), we define the group coherence $\mathbf{G_{ij}}(f)$ as follows:

$$\mathbf{G_{ij}}(f) = \frac{\sum_{x=1}^{N_i} \sum_{y=1}^{N_j} \mathbf{C_{xy}}(f)}{N_i \cdot N_j}$$

[5] EEG not organized in bursts.

References

Başar E (1980) EEG-brain dynamics: relation between EEG and brain evoked potentials. Elsevier, Amsterdam

Başar E, Demilrap T, Schürmann M, Başar-Eroglu C, Ademoglu A (1999) Oscillatory brain dynamics, wavelet analysis, ands cognition. Brain Lang 66:146–183

Browne M, Cutmore TRH (2004) Low-probability event-detection and separation via statistical wavelet thresholding: an application to psychophysiological denoising. Clin Neurophysiol 113(9): 1403–1411

Burkitt GR, Silberstein RB, Cadusch PJ, Wood AW (2000) Steady-state visual evoked potentials and travelling waves. Clin Neurophysiol 111(2):246–258

Chen Z, Ohara S, Cao J, Vialatte FB, Lenz FA, Cichocki A (2007) Statistical modeling and analysis of laser-evoked potentials of electrocorticogram recordings from awake humans. Comput Intell Neurosci 2007:10479

Chen Z, Cao J, Cao Y, Zhang Y, Gu F, Zhu G, Hong Z, Wang B, Cichocki A (2008) An empirical EEG analysis in brain death diagnosis for adults. Cogn Neurodyn 2(3):257–271

Cosmelli D, Lachaux JP, Thompson E (2007) Neurodynamical approaches to consciousness. In: Zelazo PD, Moscovitch M, Thompson E (eds) The Cambridge handbook of consciousness. Cambridge University Press, Cambridge

Cui J, Wong W (2006) The adaptive Chirplet transform and visual evoked potentials. IEEE Trans Biomed Eng 53(7):1378–1384

Dauwels J, Vialatte F, Cichocki A (2007) A novel measure for synchrony and its application to neural signals. In: Proceedings of the 32nd IEEE international conference on acoustics, speech, and signal processing (ICASSP'07), 15–20 April 2007, Honolulu, vol 4, pp 1165–1168

Dauwels J, Vialatte F, Rutkowski TM, Cichocki A (2008) Measuring neural synchrony by message passing. In: Koller D, Singer Y, Platt J (eds) Advances in neural information processing systems 20. MIT, Cambridge

Dauwels J, Vialatte F, Weber T, Cichocki A (2009) Quantifying statistical interdependance by message passing on graphs: algorithms and applications to neural signals—part A. Neural Comput (in press)

Di Russo F, Pitzalis S, Aprile T, Spitoni G, Patria F, Stella A, Spinelli D, Hillyard SA (2007) Spatiotemporal analysis of the cortical sources of the steady-state visual evoked potential. Hum Brain Mapp 28(4):323–334

Ding J, Sperling G, Srinivasan R (2006) Attentional modulation of SSVEP power depends on the network tagged by the flicker frequency. Cereb Cortex 16(7):1016–1029

Duckrow RB, Zaveri HP (2005) Coherence of the electroencephalogram during the first sleep cycle. Clin Neurophysiol 116(5): 1088–1095

Effern A, Lehnertz K, Schreiber T, David P, Elger C (2000) Nonlinear denoising of transient signals with application to event related potentials. Physica D 140:257–266

Freeman WJ (2004) Origin, structure, and role of background EEG activity. Part 1. Analytic amplitude. Clin Neurophysiol 115(9):2077–2088

Freeman WJ (2006) A cinematographic hypothesis of cortical dynamics in perception. Int J Psychophysiol 60(2):149–161

Friston KJ, Holmes AP, Worsley KJ (1999) How many subjects constitute a study? NeuroImage 10:1–5

Herrmann CS, Grigutsch M, Busch NA (2005) EEG oscillations and wavelet analysis. In: Handy T (ed) Event-related potentials: a methods handbook. MIT, Cambridge, pp 229–259

Kay SM (1998) Modern spectral estimation. Prentice-Hall, Englewood Cliffs

Kiebel SJ, Garrido MI, Moran RJ, Friston KJ (2008) Dynamic causal modelling for EEG and MEG. Cogn Neurodyn 2(2):121–136

Kim YJ, Grabowecky M, Paller KA, Muthu K, Suzuki S (2007) Attention induces synchronization-based response gain in steady-state visual evoked potentials. Nat Neurosci 10(1):117–125

Klimesch W, Sauseng P, Hanslmayr S, Gruber W, Freunberger R (2007) Event-related phase reorganization may explain evoked neural dynamics. Neurosci Biobehav Rev 31(7):1003–1016

Le Van Quyen M (2003) Disentangling the dynamic core: a research program for a neurodynamics at the large-scale. Biol Res 36(1):67–88

Le Van Quyen M, Bragin A (2007) Analysis of dynamic brain oscillations: methodological advances. Trends Neurosci 30(7): 365–373

Moratti S, Clementz B, Gao Y, Ortiz T, Keil A (2007) Neural mechanisms of evoked oscillations: stability and interaction with transient events. Hum Brain Mapp 28(12):1318–1333

Nikulin V, Linkenkaer-Hansen K, Nolte G, Lemm S, Müller K, Ilmoniemi R, Curio G (2007) A novel mechanism for evoked responses in the human brain. Eur J NeuroSci 25(10):3146–3154

Nishifuji S, Ohkado H, Tanaka S (2006) Characteristics of alpha wave response to Flicker Stimuli with color alternation. Electron Commun Jpn (part 3) 89(4) [translated from Nishifuji S, Ohkado H, Tanaka S (2005) Denshi Joho Tsushin Gakkai Ronbunshi J88-A(4):480–489]

Nunez PL, Srinivasan R (2006) Electric fields of the brain, the neurophysics of EEG. Oxford University Press, Oxford

Ohara S, Crone NE, Weiss N, Lenz FA (2004) Attention to a painful cutaneous laser stimulus modulates electrocorticographic event-related desynchronization in humans. Clin Neurophysiol 115:1641–1652

Quiroga R, Sakowitz O, Başar E, Schürmann M (2001) Wavelet transform in the analysis of the frequency composition of evoked potentials. Brain Res Protoc 8:16–24

Regan D (1989) Human brain electrophysiology: evoked potentials and evoked magnetic fields in science and medicine. Elsevier, New York

Rojas-Líbano D, Kay LM (2008) Olfactory system gamma oscillations: the physiological dissection of a cognitive neural system. Cogn Neurodyn 2(3):179–194

Schinkel S, Marwan N, Kurths J (2007) Order patterns recurrence plots in the analysis of ERP data. Cogn Neurodyn 1(4):317–325

Snyder A (1992) Steady-state vibration evoked potentials: descriptions of technique and characterization of responses. Electroencephalogr Clin Neurophysiol 3:257–268

Stapells DR, Linden D, Suffield JB, Hamel G, Picton TW (1984) Human auditory steady state potentials. Ear Hear 5(2):105–113

Tallon-Baudry C, Bertrand O, Delpuech C, Pernier J (1996) Stimulus specificity of phase-locked and non-phase-locked 40 Hz visual responses in human. J Neurosci 16(13):4240–4249

Thorpe SG, Nunez PL, Srinivasan R (2007) Identification of wave-like spatial structure in the SSVEP: comparison of simultaneous EEG and MEG. Stat Med 26(21):3911–3926

Varela F, Lachaux JP, Rodriguez E, Martinerie J (2001) The Brainweb: phase synchronization and large-scale integration. Nat Rev Neurosci 2(4):229–239

Vialatte FB, Cichocki A (2008) Split-test Bonferroni correction for QEEG statistical maps. Biol Cybern 98(4):295–303

Vialatte FB, Cichocki A, Dreyfus G, Musha T, Shishkin SL, Gervais R (2005) Early detection of Alzheimer's disease by blind source separation, time frequency representation, and bump modeling of EEG signals. In: International Conference on Artificial Neural Networks, Warsaw, Poland, 11–15 September 2005. LNCS, vol 3696. Springer, Heidelberg, pp 683–692

Vialatte F, Martin C, Dubois R, Haddad J, Quenet B, Gervais R, Dreyfus G (2007) A machine learning approach to the analysis of time-frequency maps, and its application to neural dynamics. Neural Netw 20:194–209

Vialatte F, Sole-Casals J, Dauwels J, Maurice M, Cichocki A (2008a) Bump Time Frequency toolbox software, version 1.0. Available online at: http://www.bsp.brain.riken.jp/~fvialatte/bumptoolbox/download.html

Vialatte F, Dauwels J, Rutkowski TM, Cichocki A (2008b) Oscillatory event synchrony during steady state visual evoked potentials. In: Wang R, Gu F, Shen E (eds) Advances in cognitive neurodynamics. Proceedings of the international conference on cognitive neurodynamics 2007. Springer, pp 439–442

Vialatte F, Sole-Casals J, Cichocki A (2008c) EEG windowed statistical wavelet scoring for evaluation and discrimination of muscular artifacts. Physiol Meas 29(12):1435–1452

Vialatte F, Bakardjian H, Prasad R, Cichocki A (2009) EEG paroxysmal gamma waves during Bhramari Pranayama: a yoga breathing technique. Conscious Cogn (in press)